GeroScience
https://doi.org/10.1007/s11357-026-02627-8

ORIGINAL ARTICLE

Resistant hypertension and accelerated vascular aging: evidence for PTEN–AKT-associated cellular senescence

Hang Yu · Xiaoyao Wang · Kangbo Li · Mesud Sacirovic · Oliver Ritter · Kilian Rittig · Michael Bader · Ivo Buschmann · Philipp Hillmeister

Received: 30 June 2026 / Accepted: 23 October 2026
© The Author(s) 2026

Abstract Resistant hypertension (RH) is increasingly linked to accelerated vascular aging and is particularly prevalent among older and obese individuals. Cellular senescence has emerged as a potential driver of vascular aging, but its contribution to RH remains unclear. We examined age and body mass index (BMI) in the WalkByLab cohort and assessed whether RH was associated with vascular features consistent with accelerated aging. Obesity-related transcriptomic datasets were integrated with a curated senescence-associated gene set to identify candidate regulators, followed by validation in an independent RH dataset, PBMCs, and human endothelial cells. An exploratory clinical–molecular nomogram was also developed. BMI and age increased progressively from normotension to RH. RH was characterized by reduced flow-mediated dilation, increased pulse wave index, and unchanged ankle–brachial index, consistent with endothelial dysfunction and arterial stiffness. Transcriptomic analyses identified enrichment of inflammatory, PI3K–AKT, and senescence-associated pathways. In PBMCs from RH patients, PTEN expression was reduced, AKT phosphorylation was increased, and p16/p21 levels were elevated, indicating a systemic senescence-associated molecular profile. In human endothelial cells, exposure to obese serum or pharmacological PTEN inhibition induced AKT activation and cellular senescence, whereas AKT inhibition attenuated these effects. Together,

Supplementary Information The online version contains supplementary material available at https://doi.org/10.1007/s11357-026-02627-8.

H. Yu · X. Wang · M. Sacirovic · K. Rittig · I. Buschmann · P. Hillmeister (✉)
Department for Angiology, Center for Internal Medicine I, Deutsches Angiologie Zentrum Brandenburg – Berlin (DAZB), Brandenburg Medical School Theodor Fontane, University Clinic Brandenburg, Brandenburg an der Havel, Germany
e-mail: philipp.hillmeister@mhb-fontane.de

H. Yu · M. Bader
Charité – Universitätsmedizin Berlin, Corporate Member of Freie Universität Berlin and Humboldt-Universität zu Berlin, Berlin, Germany

K. Li
School of Clinical Medicine, North China University of Science and Technology, Tangshan, China

O. Ritter
Brandenburg Medical School Theodor Fontane (MHB), Department for Cardiology, Center for Internal Medicine I, University Clinic Brandenburg, Brandenburg an der Havel, Germany

M. Bader
Max Delbrück Center for Molecular Medicine in the Helmholtz Association (MDC), Berlin, Germany

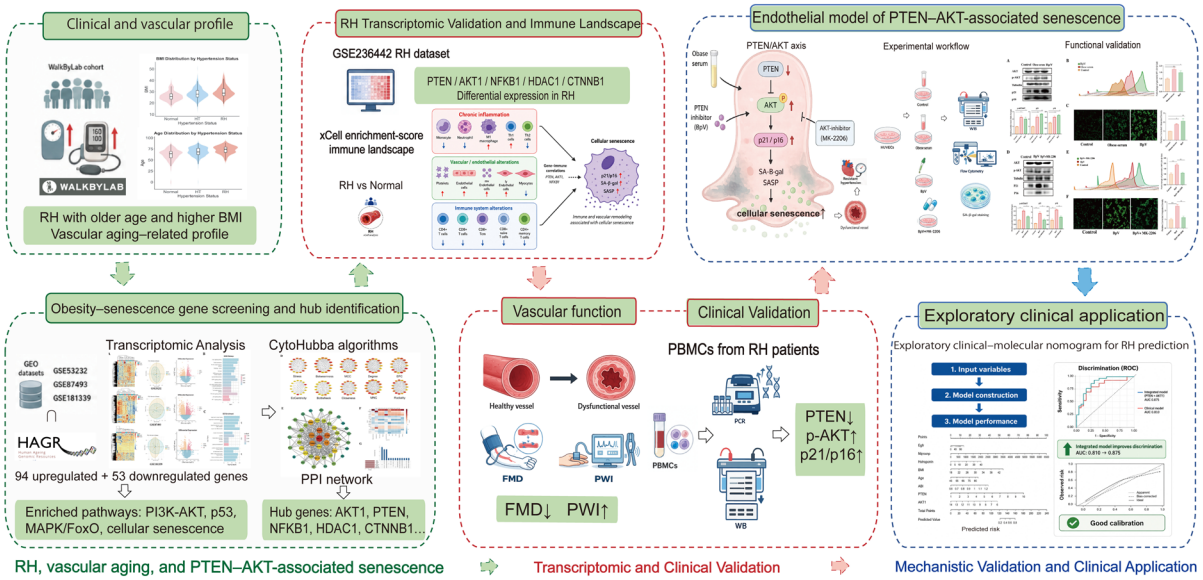
M. Bader
German Center for Cardiovascular Research (DZHK), Partner Site Berlin, Berlin, Germany

M. Bader
Institute for Biology, University of Lübeck, Lübeck, Germany

Published online: 05 November 2026

transcriptomic, clinical, and experimental findings indicate that RH is associated with vascular and molecular features consistent with accelerated vascular aging. Human data indicate a systemic senescence-associated molecular profile, whereas endothelial cell experiments support endothelial senescence as a mechanistically relevant cellular component. PTEN–AKT-associated cellular senescence may represent one mechanistically relevant component linking obesity to vascular dysfunction in RH.

Graphical Abstract



Keywords Resistant hypertension · Endothelial dysfunction · Cellular senescence · PTEN · AKT · Vascular aging

Introduction

Resistant hypertension is defined as blood pressure that remains uncontrolled despite the use of three different classes of antihypertensive agents, including a diuretic, at optimal or maximal tolerated doses, or blood pressure that can only be controlled with four or more medications. Epidemiological data show that, after excluding measurement bias due to the "white-coat effect" and poor medication adherence, resistant hypertension still accounts for approximately 10% of all hypertension cases, affecting an estimated 100 to 500 million individuals worldwide [1, 2]. Patients with resistant hypertension are at a markedly higher risk of developing heart failure, end-stage renal disease, and ischemic heart disease, posing a significant global public health burden [3]. Beyond its operational definition by treatment failure, RH is frequently accompanied by vascular abnormalities such as endothelial dysfunction and arterial stiffening [4, 5]. Notably, RH occurs more frequently in older and obese individuals, raising the possibility that accelerated vascular aging may contribute to its clinical and vascular characteristics. Given its distinct clinical profile, RH may involve biological mechanisms beyond those driving essential hypertension.

Endothelial dysfunction, arterial stiffening, oxidative stress, and cellular senescence are also recognized features of vascular aging [6]. A growing body of evidence has established cellular senescence

I. Buschmann · P. Hillmeister
Faculty of Health Sciences Brandenburg, Joint Faculty of the Brandenburg University of Technology Cottbus – Senftenberg, the Brandenburg Medical School Theodor Fontane, University of Potsdam, Brandenburg an der Havel, Germany

as one of the key drivers of vascular aging [7]. Cellular senescence refers to a state in which metabolically active cells undergo irreversible growth arrest, accompanied by phenotypic alterations such as cellular hypertrophy, chromatin remodeling, and telomere shortening. Among these, endothelial cell senescence is particularly associated with vascular dysfunction [8]. Senescent endothelial cells typically exhibit enlarged morphology, altered shape, increased reactive oxygen species (ROS) production, and the acquisition of a senescence-associated secretory phenotype (SASP). These alterations lead to reduced vascular density, increased intimal thickness, excessive collagen deposition, decreased elastin content, and ultimately vascular inflammation, aortic stiffness, and impaired vasomotor regulation—all of which are key contributors to hypertension [9, 10]. Cellular senescence does not occur in isolation. Chronic low-grade inflammation, age-related immune dysregulation, and oxidative stress may reinforce senescence-associated vascular changes and sustain a pro-inflammatory vascular environment. At the same time, declining endothelial resilience may increase the susceptibility of the aging vasculature to persistent hemodynamic and metabolic stress [11, 12]. These concepts represent established senescence biology and provide a framework for examining, rather than presuming, its involvement in RH. However, the extent to which these processes are involved in RH remains poorly understood. Whether RH is associated with vascular and molecular features consistent with accelerated vascular aging, and whether senescence-related pathways contribute to these features, remain largely unknown.

Obesity may accelerate vascular aging through chronic low-grade inflammation, oxidative stress, adipokine imbalance, and metabolic stress, all of which can promote cellular senescence and impair vascular homeostasis. Thus, older age and obesity may represent complementary contributors to vascular aging. Interestingly, our WalkByLab cohort study revealed that obesity, aging, and resistant hypertension frequently coexist, raising the possibility that vascular aging-related processes may be particularly relevant in RH. To explore molecular mechanisms that may connect obesity and aging with vascular aging processes in RH, we integrated publicly available transcriptomic datasets related to obesity and aging and performed network-based analyses to identify genes positioned at the intersection of these processes, revealing a proinflammatory milieu and highlighting cellular senescence and vascular dysfunction as key processes. Among the regulators highlighted by these analyses, PTEN (Phosphatase and Tensin Homolog deleted on chromosome 10) emerged as a potential mechanistic link. PTEN links to cellular senescence and vascular aging, yet it is not a canonical senescence marker. Rather, PTEN functions as a regulator of multiple pathways, acting upstream of obesity- and aging-related signaling networks identified in our transcriptomic analyses, and may therefore represent a regulatory node through which metabolic stress and vascular dysfunction converge.

There are several biological reasons supporting PTEN as a plausible mechanistic link between obesity, vascular aging, and resistant hypertension. PTEN is a central negative regulator of PI3K/AKT signaling and plays critical roles in metabolic homeostasis, vascular remodeling, and endothelial function [13, 14]. Through the inhibition of PI3K/AKT signaling, PTEN modulates vascular cell proliferation, migration, metabolism, and reactivity, thereby influencing vascular remodeling, endothelial function, and regulation of vascular tone [15]. Importantly, the PI3K/AKT pathway directly regulates endothelial nitric oxide synthase (eNOS) activity and nitric oxide (NO) bioavailability, which are essential determinants of endothelium-dependent vasodilation. At the same time, PTEN activity is highly sensitive to metabolic and inflammatory conditions. Obesity-associated chronic low-grade inflammation and oxidative stress have been shown to modulate PTEN expression and activity through multiple mechanisms, thereby altering downstream PI3K/AKT signaling and vascular insulin sensitivity [16, 17].

Taken together, these observations led us to hypothesize that obesity-associated metabolic stress may contribute to vascular aging-related changes in resistant hypertension through dysregulation of PTEN signaling, with consequent AKT activation, endothelial senescence-related changes, and vascular dysfunction.

Methods

Datasets related to senescence, obesity, and hypertension

The senescence-associated gene dataset used in this study was obtained from the Human Ageing Genomic

Resources (HAGR, https://genomics.senescence.info/). Microarray data related to obesity were downloaded from the NCBI Gene Expression Omnibus (GEO, https://www.ncbi.nlm.nih.gov/geo/). A total of three human microarray datasets were included: GSE53232, GSE87493, and GSE181339. These datasets represent independent human cohorts generated on different platforms and tissues, including PBMCs, whole blood–derived transcriptome, and adipose tissue. Because obesity is a systemic metabolic disorder involving immune activation, metabolic dysregulation, and vascular dysfunction, the inclusion of datasets from different tissues may help capture shared transcriptional signatures rather than tissue-specific expression patterns. In addition, an RNA-sequencing (RNA-seq) dataset associated with resistant hypertension, GSE236442, was incorporated. This dataset was generated on the GPL24676 platform and includes 10 control samples and 10 samples from patients with resistant hypertension. The sample sources, array platforms, and case–control compositions of these datasets are summarized in Table 1.

Screening and analysis of high-potential genes

Normalized expression matrices from the GSE53232, GSE87493, and GSE181339 microarray datasets were downloaded and annotated. Because the datasets were generated on different microarray platforms, each dataset was analyzed independently to avoid potential cross-platform batch effects. To minimize treatment-related variability, only baseline obese and baseline control samples were included. Differential expression analysis was performed using the limma package in R with empirical Bayes moderation. For exploratory candidate discovery, genes with nominal $P < 0.05$ were retained as potential obesity-associated signals and visualized using heatmaps and volcano plots generated by the heatmap and ggplot2 packages. These genes were treated as candidate signals and were subsequently prioritized through senescence-gene intersection and downstream validation analyses. Candidate gene lists from the three datasets were then integrated using a union-based approach and intersected with the list of cellular senescence-related genes obtained from the Human Ageing Genomic Resources (HAGR, https://genomics.senescence.info/) to derive the set of high-potential genes. Gene Ontology (GO) and Kyoto Encyclopedia of Genes and Genomes (KEGG) pathway enrichment analyses were performed using the "GOplot" package. GO analysis included three major categories: cellular components (CC), biological processes (BP), and molecular functions (MF).

Protein–protein interaction network construction and hub gene identification

The PPI network of high-potential genes was constructed using the STRING database (https://string-db.org/) with the default "medium" confidence threshold. The network was visualized and analyzed using Cytoscape software (version 3.9.0). The "CytoHubba" plugin was applied to calculate ten centrality

Table 1 Summary of public gene expression datasets used in this study

ID	Platform	Normal	Obese	Total	Notes
GSE53232	GPL11532 – Affymetrix Human Gene 1.1 ST	17	15	32	Only baseline PBMC samples from the two subject groups were used
GSE87493	GPL6244 – Affymetrix Human Gene 1.0 ST	20	12	32	Peripheral blood
GSE181339	GPL20844 – Agilent SurePrint G3 Human GE v3	12	12	24	Only baseline Adipose tissue samples from the two subject groups were retained
ID	**Platform**	**Normal**	**RH**	**Total**	**Notes**
GSE236442	GPL24676 – Illumina NovaSeq 6000	10	10	20	Whole blood

Summary of the publicly available datasets included in the analysis. Each dataset was downloaded from the Gene Expression Omnibus (GEO) database and processed for differential gene expression analysis as described in the Methods section

indices—Degree, MCC, MNC, EPC, Bottleneck, Eccentricity, Closeness, Betweenness, Radiality, and Stress. For each metric, the top 15 genes with the highest scores were selected, and the intersection of these ten lists was defined as the consensus hub genes. The intersections were visualized using the "UpSetR" package, and the relative centrality scores of the top 15 hub genes across the ten algorithms were displayed as a heatmap using the "pheatmap" package.

Validation and immune infiltration analysis of high-potential genes

An independent RNA-seq dataset (GSE236442) was downloaded from the GEO database. Differential gene expression between the resistant hypertension group and the control group was analyzed using the "limma" package, and the significance of candidate hub genes was evaluated based on adjusted P-values (adj.P.Val). Results were visualized as violin plots generated by "ggplot2". The enrichment scores of 64 immune and stromal cell types were estimated using the xCell algorithm (v1.3.0) under default parameters. xCell provides relative enrichment scores rather than absolute cell proportions, allowing inference of cell-type–associated transcriptional signals across samples. Differences in enrichment scores between groups were compared using the Wilcoxon rank-sum test, and P values were adjusted for multiple testing using the Benjamini–Hochberg false discovery rate method; adjusted $P < 0.05$ was considered statistically significant. Heatmaps of cell-type enrichment scores were produced using "pheatmap". Differentially enriched immune cell types were visualized using the "forestplot" function. Spearman's correlation coefficients between candidate gene expression levels and immune cell enrichment scores were calculated, and the results were visualized as a correlation matrix using "corrplot". Gene–cell interaction networks were further illustrated with chord diagrams generated by the "circlize" package.

Construction of the nomogram

To identify key predictors of RH, all clinically relevant variables, including demographic factors, renal and cardiac biomarkers, vascular indicators, and molecular markers, were analyzed. Least absolute shrinkage and selection operator (LASSO) logistic regression was applied to select the most informative predictors while reducing model overfitting. Tenfold cross-validation was used to determine the optimal regularization parameter (λ) that minimized binomial deviance. Variables with nonzero coefficients at the optimal λ were retained to build the final multivariable logistic regression model. A nomogram was then constructed using the "rms" package in R software to visualize the model and estimate the individual probability of RH. Model discrimination was assessed using the area under the receiver operating characteristic curve (AUC), and calibration was evaluated by calibration plots with 1,000 bootstrap resamples. Due to the availability of molecular data, the predictive modeling and correlation analyses were performed in a subset of patients with complete gene expression information. The number of predictors retained in the final model was limited to reduce the risk of model overfitting.

Participants and clinical characteristics

A total of 821 patients were initially identified from the WalkByLab Center Brandenburg/Havel (www.lauflab.de) of the Brandenburg Clinic, Brandenburg Medical School. RH was defined as blood pressure remaining above target despite treatment with three antihypertensive agents of different classes, including a diuretic, or blood pressure controlled only with four or more medications. Blood pressure measurements and antihypertensive treatment information were obtained from routine clinical records. When available, out-of-office blood pressure data were reviewed to reduce potential misclassification related to the white-coat effect. Molecular analyses and clinical–molecular modeling were performed in subsets of participants according to data availability. The WalkByLab registry study protocol was reviewed and approved by the Ethics Committee of the State Medical Association of Cottbus (Landesärztekammer Cottbus, Ethics Approval No. AS 74(bB)/2018). All procedures were conducted in accordance with the principles of the Declaration of Helsinki. Demographic and clinical characteristics of the study participants are summarized in Table 2.

Assessment of vascular function

Vascular function was assessed using three non-invasive parameters: flow-mediated dilation (FMD, %), pulse wave index (PWI, a.u.), and oscillometric ankle–brachial index (ABI, ratio). FMD was measured with the AngioDefender™ system (Everist Health), which provides automated oscillometric assessment of endothelial function and has been validated against Doppler ultrasound–based FMD measurements. PWI and ABI were obtained using the AngE Pro8 device (SYCO MeData GmbH), which employs oscillometry to derive pulse wave amplitude and timing parameters, allowing standardized evaluation of vascular stiffness and peripheral perfusion. Group differences in vascular function were first compared using unadjusted analyses. To account for potential confounding by age, linear regression models were further applied with age as a covariate. Statistical significance was defined as $P < 0.05$.

Isolation of peripheral blood mononuclear cells (PBMCs)

Peripheral venous blood samples (10 mL) were collected from each participant in ethylenediaminetetraacetic acid (EDTA)-coated vacuum tubes. PBMCs were isolated using Ficoll-Paque™ PLUS density gradient medium (Cytiva). Briefly, the blood samples were centrifuged at 1000 × g for 10 min, and the plasma was collected and stored at − 80 °C. The remaining samples were diluted 1:1 with phosphate-buffered saline (PBS) and carefully layered at a 4:3 ratio onto Ficoll-Paque™ PLUS medium, followed by centrifugation at 1000 × g for 15 min. The interphase layer containing PBMCs was collected, washed twice with PBS, and resuspended in cryopreservation solution (Gibco) before storage at − 80 °C.

RNA extraction and quantitative real-time polymerase chain reaction (qRT-PCR)

Total RNA was extracted from PBMCs using TRIzol reagent (Thermo Fisher Scientific) according to the manufacturer's instructions. The extracted RNA was reverse-transcribed into complementary DNA (cDNA) using the ABclonal Reverse Transcription Kit (ABclonal). Quantitative real-time PCR (qRT-PCR) was performed using the QuantStudio™ 7 Pro Real-Time PCR System. The relative mRNA expression levels of target genes were calculated using the $2^{-}\Delta\Delta$Ct method. All primers were synthesized by Eurofins Genomics Germany GmbH. PBMC-based qRT-PCR analyses were performed in participants with available high-quality RNA. Samples with reference gene Ct values > 25 were excluded according to predefined quality-control criteria, consistent with the criteria reported in Fig. 4.

Table 2 Baseline characteristics of study participants from the WalkByLab cohort

Variables	Non-Hypertension ($n = 228$)	Hypertension ($n = 427$)	Resistant Hypertension ($n = 166$)	P value
Age, years	61.9 ± 12.4	68.3 ± 10.2	72.6 ± 8.9	< 0.001
Male, n (%)	111 (48.7)	266 (62.3)	60 (36.1)	< 0.001
BMI, kg/m^2	25.9 ± 4.1	28.3 ± 4.8	29.8 ± 4.7	< 0.001
Current/ex-smokers, n (%)	89 (39.0)	205 (48.0)	66 (39.8)	0.0434
HbA1c, %	5.69 ± 0.53	6.09 ± 0.46	6.30 ± 0.96	< 0.001
eGFR, mL/min/1.73 m^2	85.8 [72.1–95.6]	75.2 [60.7–88.5]	64.8 [51.6–78.4]	< 0.001
Creatinine, µmol/L	76.0 ± 28.6	86.0 ± 34.4	98.0 ± 39.5	< 0.001
NT-proBNP, pg/mL	280.7 [69.5–2326.6]	307.5 [144.5–487.8]	642.3 [285.0–947.5]	< 0.001
hs-Troponin, ng/L	8.2 [4.1–13.6]	13.7 [6.2–21.5]	19.3 [8.8–36.0]	< 0.001

Baseline demographic and biochemical characteristics of participants in the WalkByLab Brandenburg cohort. Data are presented as mean ± SD for normally distributed variables or median [IQR] for skewed variables. P values indicate group comparisons by one-way ANOVA or the Kruskal–Wallis test for continuous variables, and by the chi-square test or Fisher's exact test for categorical variables, as appropriate

Cell culture and treatments

Human umbilical vein endothelial cells (HUVECs) were maintained at 37 °C and 5% CO_2 in DMEM/F12 supplemented with 10% fetal bovine serum (FBS), 100 U/mL penicillin, and 100 µg/mL streptomycin. Cells were divided into four groups: (1) Control: cells were maintained in standard culture medium containing 10% FBS, which served as the baseline growth condition. (2) Obese-serum: cells were cultured in medium containing 5% FBS supplemented with 5% pooled human serum obtained from obese donors (BMI ≥ 30 kg/m^2) to introduce circulating metabolic factors while maintaining comparable basal culture conditions. (3) BpV: cells were treated with the PTEN inhibitor bisperoxovanadium (BpV, 1 µM) for 24 h. (4) BpV + MK-2206: cells were co-treated with BpV (1 µM) and the AKT inhibitor MK-2206 (2 µM) for 24 h to assess whether AKT inhibition could reverse PTEN-loss–induced effects.

Obese human serum used for endothelial cell stimulation was obtained from adult volunteers with obesity (BMI ≥ 30 kg/m^2) recruited from the WalkByLab cohort. Serum donors were screened to exclude acute infection, malignant disease, and systemic inflammatory disorders. To minimize inter-individual variability, serum samples from multiple donors were pooled prior to use. Equal volumes of serum from each donor were combined to generate a pooled obese-serum batch. The pooled serum was filtered through a 0.22 µm filter, aliquoted, and stored at − 80 °C until use. After treatments, cells were collected for Western blotting, fluorescence microscopy, and flow cytometry.

Western blot analysis

Total protein was extracted using RIPA buffer (Thermo Fisher Scientific). Protein concentration was quantified using the BCA kit (Taoshu). Equal protein amounts were separated by 10% SDS–PAGE, transferred to 0.22 µm PVDF membranes (Millipore), and blocked for 40 min at room temperature. Membranes were incubated overnight at 4 °C with primary antibodies (1:1000), followed by HRP-conjugated secondary antibodies (1:10,000, 1 h, room temperature). Primary antibodies: PTEN, AKT, phospho-AKT (Ser473), p16, p21, α-tubulin, GAPDH (ABclonal). Detection used an ECL kit (Thermo Fisher Scientific) and a VWR imaging system. For PBMC Western blot validation, a smaller subset of normotensive and RH participants with sufficient PBMC protein yield and comparable sample quality was used. For cell-culture experiments, biological replicates refer to independently treated and processed cell cultures. Unless otherwise indicated, in vitro experiments were repeated at least three times independently.

Detection of cellular senescence

Cellular senescence was evaluated by fluorescence microscopy and flow cytometry. Cryopreserved cells were thawed, washed, and cultured for 18 h in complete medium. For microscopy, senescence-associated β-galactosidase (SA-β-gal) activity was measured using the CellEvent™ Senescence Green Detection Kit (Thermo Fisher Scientific) and imaged with a Leica STELLARIS STED confocal microscope. Images were acquired using a 10× objective with identical microscope settings within each experiment. For each condition, fluorescence intensity was quantified from three randomly selected fields per biological replicate using ImageJ software. Mean fluorescence intensity was calculated after background subtraction and normalized to the control condition. For flow cytometry, the CellEvent™ Senescence Green Flow Cytometry Assay Kit (Thermo Fisher Scientific) was used per manufacturer's instructions, analyzed on a BD flow cytometer with FlowJo software. Debris and doublets were excluded based on FSC/SSC and FSC-A/FSC-H gating. A minimum of 10,000 events was acquired per sample, and the same gating strategy was applied across all samples. SA-β-gal activity was quantified as mean fluorescence intensity (MFI) and normalized to the control condition.

Statistical analysis

Statistical analyses were performed using GraphPad Prism 9 and R software (4.5.0). For comparisons between two independent groups, continuous variables were first tested for normality. If the data followed a normal distribution with equal variances, a two-tailed Student's t-test was applied; otherwise, the Mann–Whitney U test (also known as the Wilcoxon rank-sum test) was used. For comparisons among three groups, normally distributed continuous variables were analyzed using one-way

ANOVA, whereas non-normally distributed variables were analyzed using the Kruskal–Wallis test. Categorical variables were compared using the chi-square test or Fisher's exact test, as appropriate. For in vitro experiments involving multiple groups, one-way ANOVA followed by Tukey's multiple-comparisons test was used. A p-value ≤ 0.05 was considered to indicate statistical significance.

Results

Association of BMI and age with resistant hypertension

To determine whether clinical characteristics could provide initial insights into vascular aging-related features in RH, we first examined how age and body mass index (BMI) differ across blood pressure categories. There were significant differences in the distribution of BMI and age among the normotensive, hypertensive, and resistant hypertension groups. Violin plots demonstrated that both BMI and age were higher in the RH group than in the hypertension (HT) and Normal groups, showing a clear increasing trend across the three populations (Fig. 1a and b). Locally estimated scatterplot smoothing (LOESS) curves indicated that both age and BMI were positively associated with the risk of hypertension, with an increase in risk observed among individuals aged > 60 years and those with BMI > 28 kg/m^2 (Fig. 1c and d). The generalized additive model (GAM) further revealed a nonlinear association, confirming that the risk of hypertension increased significantly within these ranges ($P < 0.05$; Fig. 1e and f). Multivariate logistic regression analysis further supported these findings (Fig. 1g). Compared with the Normal group, age was significantly associated with an increased risk of both HT and RH. Although BMI was also significantly associated with HT, it appeared more pronounced in RH. These findings indicate that RH is enriched for older age and higher BMI, two clinical features closely related to metabolic stress and vascular aging, providing a rationale for further investigation of senescence- and vascular dysfunction-related mechanisms.

Identification of candidate genes and functional enrichment analysis

To investigate potential biological pathways underlying these clinical associations, we performed an exploratory transcriptomic screening using public obesity-related gene expression datasets. Because obesity is a major risk contributor to metabolic stress and vascular aging, we aimed to identify genes linking obesity-associated transcriptional alterations with cellular senescence pathways, which may contribute to vascular dysfunction in RH. We first identified candidate obesity-associated genes in the GSE53232, GSE87493, and GSE181339 datasets. These candidate genes were subsequently integrated across datasets and intersected with a curated list of senescence-associated genes to obtain a set of high-potential regulators. For each dataset, heatmap visualization and principal component analysis (PCA) were performed to assess overall gene expression profiles and sample clustering. Heatmap visualization revealed distinguishable expression patterns between the normal and disease groups. PCA plots showed partial separation between groups along the first two principal components, although some overlap remained, likely reflecting biological heterogeneity across samples. Volcano plots were used to visualize up- and downregulated genes, highlighting the distribution of candidate genes across datasets (Fig. 2a). After integrating candidate gene lists from the three datasets using a union-based approach and removing duplicates, 94 upregulated and 53 downregulated candidate genes were retained for downstream analyses. KEGG pathway enrichment analysis demonstrated that candidate genes were primarily enriched in signaling pathways related to cellular stress response, aging, and metabolic homeostasis, including the HIF-1, p53, PI3K–Akt, MAPK and FoxO signaling pathways, as well as cellular senescence, autophagy, and lipid and atherosclerosis-related pathways (Fig. 2b). GO enrichment analysis further showed that, in biological processes (BP), candidate genes were mainly involved in the response to oxygen levels, hypoxia, p53-mediated signaling, and myeloid cell differentiation. In the cellular component (CC) category, they were enriched in the nuclear chromosome, spindle, transcription repressor complex, and plasma membrane raft, while molecular function (MF) enrichment included serine/threonine kinase activity, phosphatase

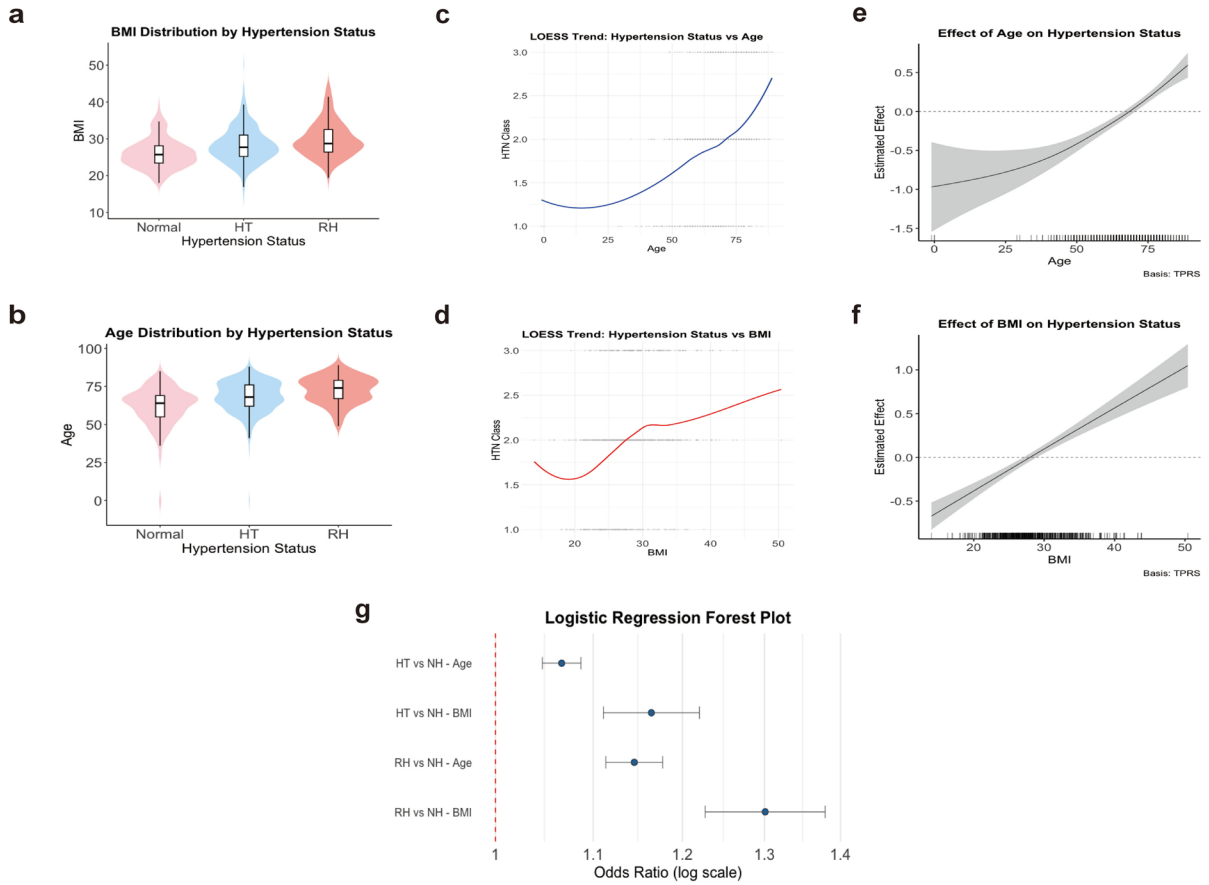
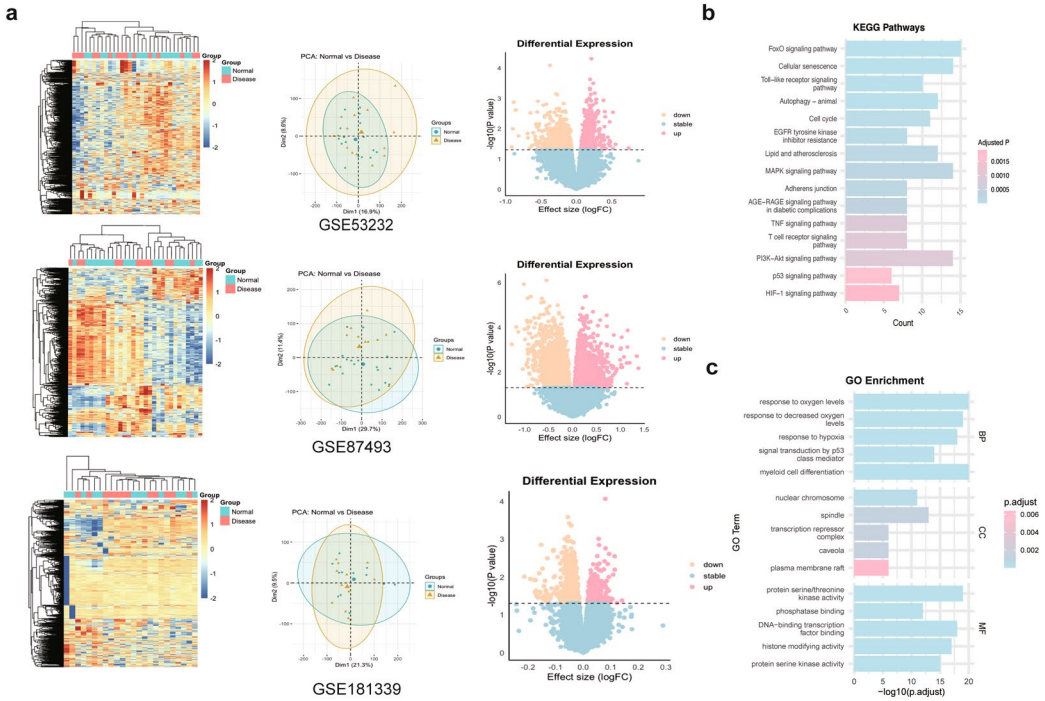


Fig. 1 Distributions and modeling of BMI and age across hypertension status. **a**–**b** Violin plots showing the distributions of body mass index (BMI) (**a**) and age (**b**) among normotensive (Normal), hypertensive (HT), and resistant hypertension (RH) groups. **c**–**d** LOESS curves illustrating the relationships between hypertension status and age (**c**) or BMI (**d**). **e**–**f** Generalized additive model (GAM) plots showing the estimated effects of age (**e**) and BMI (**f**) on hypertension status with 95% confidence intervals. **g** Forest plot of multivariable logistic regression analyses for age and BMI across the three hypertension groups

binding, and DNA-binding transcription factor activity (Fig. 2c). Together, these findings suggest that obesity-associated transcriptional alterations converge on pathways related to cellular stress, senescence, metabolic regulation, and cardiovascular dysfunction.

PPI network construction and identification of hub genes

To further identify upstream regulatory nodes within these pathways, we constructed a PPI network to pinpoint genes with central roles in obesity- and aging-related signaling. The resulting network revealed extensive interconnectivity among encoded proteins, implying close functional relationships (Fig. 2e). To identify key regulatory genes, ten distinct topological algorithms were applied using the CytoHubba plugin, including Stress, Betweenness, Closeness, Eccentricity, Bottleneck, EPC, MCC, Degree, MNC, and Radiality (Fig. 2d). Among the intersecting results, AKT1, NFKB1, PTEN, HDAC1, CTNNB1, EP300, BRCA1, ERBB2, and UBB consistently ranked among the top nodes across multiple centrality measures, indicating their potential roles as hub regulators. The integration of the results through UpSet plot and heatmap visualization (Fig. 2f and g) further confirmed that these genes were repeatedly prioritized by multiple algorithms, reinforcing their robustness and highlighting their central roles in obesity- and aging-related pathways.


a
Group
Normal
Disease
PCA: Normal vs Disease
Groups
Normal
Disease
Dim1 (16.9%)
Dim2 (8.6%)
GSE53232
Differential Expression
-log10(P value)
Effect size (logFC)
down
stable
up
Dim1 (29.7%)
Dim2 (11.4%)
GSE87493
Dim1 (21.3%)
Dim2 (8.6%)
GSE181339
b
KEGG Pathways
FoxO signaling pathway
Cellular senescence
Toll-like receptor signaling pathway
Autophagy – animal
Cell cycle
EGFR tyrosine kinase inhibitor resistance
Lipid and atherosclerosis
MAPK signaling pathway
Adherens junction
AGE-RAGE signaling pathway in diabetic complications
TNF signaling pathway
T cell receptor signaling pathway
PI3K-Akt signaling pathway
p53 signaling pathway
HIF-1 signaling pathway
Adjusted P
0.0015
0.0010
0.0005
Count
c
GO Enrichment
response to oxygen levels
response to decreased oxygen levels
response to hypoxia
signal transduction by p53 class mediator
myeloid cell differentiation
nuclear chromosome
spindle
transcription repressor complex
caveola
plasma membrane raft
protein serine/threonine kinase activity
phosphatase binding
DNA-binding transcription factor binding
histone modifying activity
protein serine kinase activity
GO Term
BP
CC
MF
p.adjust
0.006
0.004
0.002
−log10(p.adjust)
d
Stress
Betweenness
MCC
Degree
EPC
EcCentricity
BottleNeck
Closeness
MNC
Radiality
e
GDF11
DDIT3
CCN2
CDK7
EEF1A1
CDKN2B
CDC42
UBB
ERBB2
MLH1
EIF5A2
VCP
IL7
CHEK2
PPM1D
HMGB1
NFKB1
SOD2
ERCC4
PLCG2
IFNB1
EP300
PTEN
AKT1
FOXO4
SDHC
CTNNB1
IL6
RAD52
MAP3K5
PTK2B
PTGS2
HDAC1
PAPPA
FOXO1
IGF1R
MXI1
RICTOR
IL2
MSRA
BRCA1
PCNA
SIRT7
SOD1
PDPK1
TRPV1
f
Top 15 Hub Genes (Z-score normalized, No Clustering)
AKT1
CTNNB1
PTEN
NFKB1
HDAC1
FOXO1
UBB
ERBB2
CHEK2
BRCA1
EP300
IL6
IGF1R
CDC42
PTGS2
Gene
Z-score
Betweenness
BottleNeck
Closeness
Degree
EcCentricity
EPC
MCC
MNC
Radiality
Stress
Algorithm
g
Intersection Size
MCC
Stress
Radiality
MNC
EPC
EcCentricity
Degree
Closeness
BottleNeck
Betweenness
Set Size

◂**Fig. 2** Identification and functional analysis of candidate obesity- and senescence-related genes. **a** Heatmaps, PCA plots, and volcano plots showing candidate obesity-associated genes in the GSE53232, GSE87493, and GSE181339 datasets comparing normal and disease groups. **b** KEGG pathway enrichment of overlapping candidate genes. **c** GO enrichment analysis of candidate genes, including BP, CC, and MF categories. **d** Identification of hub genes using 10 CytoHubba algorithms (Stress, Betweenness, MCC, Degree, EPC, Eccentricity, Bottleneck, Closeness, MNC, and Radiality). **e** Integrated PPI network highlighting top hub genes. **f** Heatmap of the top 15 hub genes ranked across the 10 algorithms. **g** UpSet plot showing intersections of hub genes identified by different algorithms

Immune landscape in resistant hypertension of hub genes

To explore the potential immunological mechanisms associated with the identified hub genes, immune cell infiltration analysis was performed using the xCell algorithm based on the GSE236442 transcriptome dataset. The xCell heatmap revealed distinct immune cell distribution patterns between the resistant hypertension and normal groups (Fig. 3a). Quantitative comparison of cell-type enrichment scores revealed pronounced alterations in multiple immune cell types among RH patients (Fig. 3b). RH samples showed altered enrichment scores across multiple innate and adaptive immune-cell signatures. M1 macrophage and Th1-cell enrichment scores were higher, whereas monocyte, neutrophil, and Th2-cell enrichment scores were lower in RH. In addition, endothelial cell, microvascular endothelial cell, lymphatic endothelial cell, and platelet-associated transcriptional signals were higher in the RH group, whereas myocyte-associated signals were lower. Enrichment scores for several CD4 + and CD8 + T-cell subsets were also lower in RH, further indicating altered adaptive immune-related transcriptional signatures. The chord diagram illustrated complex interconnections between hub genes and distinct immune cell populations, highlighting the broad regulatory impact of these genes on the immune microenvironment. Among them, PTEN, HDAC1, and CTNNB1 displayed negative correlations with proinflammatory M1 macrophages and endothelial cells, but positive correlations with several T-cell subsets. In contrast, AKT1 showed a positive correlation with proinflammatory cell populations. These results were further supported by the correlation heatmap, which showed consistent association patterns across all samples (Fig. 3c and d). Taken together, these findings indicate an altered immune and vascular transcriptional landscape in RH, characterized by immune dysregulation and endothelial-associated changes.

Validation of hub genes in independent cohorts and clinical samples

To validate the identified hub genes, differential expression analysis was performed using the GSE236442 transcriptomic dataset. Violin plots demonstrated that several genes, including AKT1, HDAC1, PTEN, NFKB1, EP300, CTNNB1, and ERBB2, were significantly differentially expressed between the RH and control groups (Fig. 4a). Further validation was conducted using PBMCs from the WalkByLab Brandenburg cohort. Quantitative RT–PCR analysis confirmed that PTEN expression was significantly reduced in patients with RH compared with normotensive controls, whereas AKT1 expression showed no significant difference (Fig. 4b). At the protein level, Western blot analysis revealed a marked decrease in PTEN accompanied by an increase in p-AKT in the RH group (Fig. 4c), consistent with enhanced AKT activation in PBMCs.

To determine whether this molecular alteration was associated with a senescence-related molecular profile, the expression of p21 and p16, two canonical markers of cellular senescence, was examined. Both proteins were markedly upregulated in the RH group (Fig. 4d), suggesting activation of senescence-associated molecular pathways. Vascular function was then evaluated to determine whether these molecular alterations were accompanied by functional evidence of vascular aging. After adjustment for age using a linear regression model, RH patients exhibited higher PWI and lower FMD, whereas ABI remained unchanged (Fig. 4e). Together, RH patients exhibited a systemic senescence-related molecular profile alongside vascular abnormalities consistent with vascular aging, including impaired endothelium-dependent vasodilation and increased arterial stiffness, while the unchanged ABI argued against advanced peripheral arterial obstruction.

Functional validation of PTEN/AKT signaling in endothelial senescence

To functionally validate the role of PTEN/AKT signaling in endothelial senescence, HUVECs were

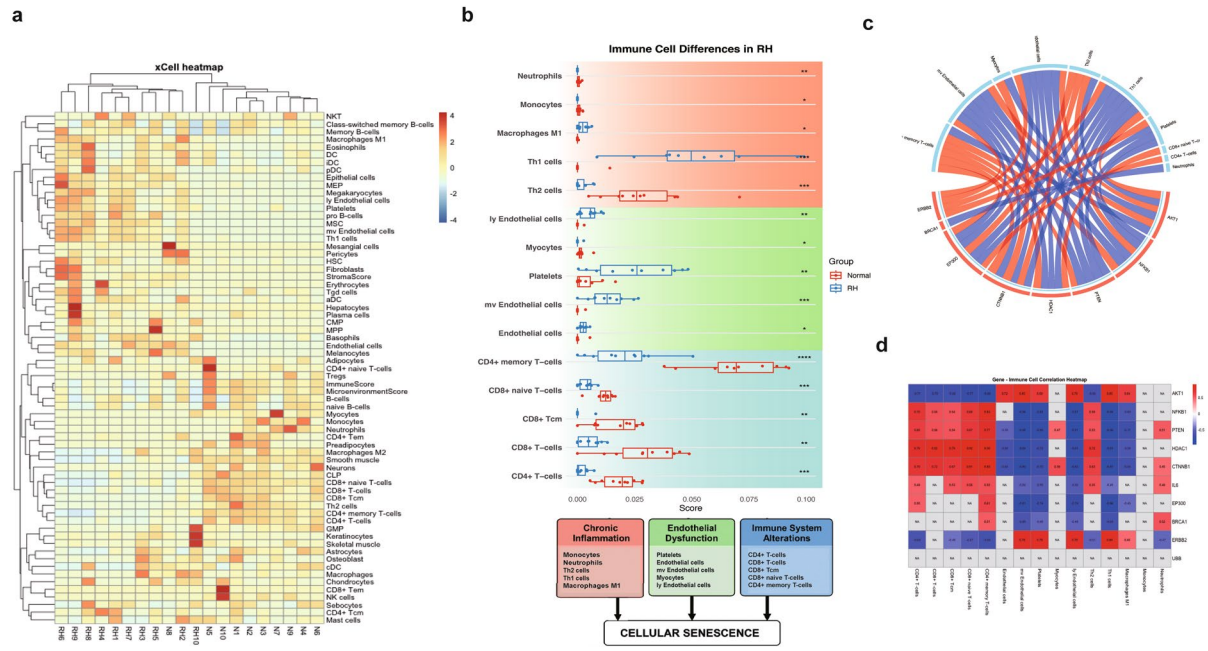


Fig. 3 Immune landscape and correlation analysis of hub genes in resistant hypertension. **a** xCell heatmap showing cell-type enrichment scores in Control and RH groups (Control $n = 10$, RH $n = 10$). **b** Boxplots comparing differential cell-type enrichment scores between normal and RH groups, with significance levels indicated. **c** Chord diagram illustrating correlations between hub genes and immune cell types. **d** Correlation heatmap showing relationships between hub gene expression levels and representative xCell enrichment scores. Spearman correlation coefficients were calculated to assess associations between hub gene expression and xCell enrichment scores. * adjusted $P < 0.05$; ** adjusted $P < 0.01$; *** adjusted $P < 0.001$; ns, non-significant

exposed to obese human serum or the PTEN inhibitor BpV. Western blotting showed that both obese-serum exposure and pharmacological PTEN inhibition enhanced AKT phosphorylation, accompanied by increased expression of senescence markers p21 and p16 (Fig. 5a). Flow cytometry further confirmed a significant elevation in β-galactosidase–positive senescent cells (Fig. 5b), and fluorescence microscopy imaging revealed intensified senescence-associated fluorescence (Fig. 5c). These findings suggest that obesity-related stimuli and pharmacological PTEN inhibition are associated with AKT activation and endothelial senescence–like phenotypes.

To determine whether AKT mediates these effects, HUVECs were co-treated with BpV and the AKT inhibitor MK-2206. Compared with BpV alone, MK-2206 co-treatment suppressed p-AKT phosphorylation and partially reversed the upregulation of p21 and p16 (Fig. 5d). Consistently, both β-galactosidase activity and senescence-associated fluorescence were reduced (Fig. 5e and f). These findings suggest that AKT signaling may contribute to the senescence phenotype observed following pharmacological PTEN inhibition. Importantly, these endothelial-cell findings are consistent with our clinical observations showing reduced PTEN expression and increased AKT phosphorylation in RH patients. Together, these results support the potential involvement of the PTEN–AKT axis in endothelial senescence and vascular dysfunction in obesity-related resistant hypertension.

Nomogram for predicting resistant hypertension

To further investigate the predictive value of the identified markers, we integrated gene expression profiles with clinical parameters to construct an exploratory nomogram model for estimating the risk of resistant hypertension. LASSO regression was applied to select the most informative features from all candidate variables. Several predictors with non-zero coefficients were retained, including both clinical and molecular indicators (Fig. 6b). These

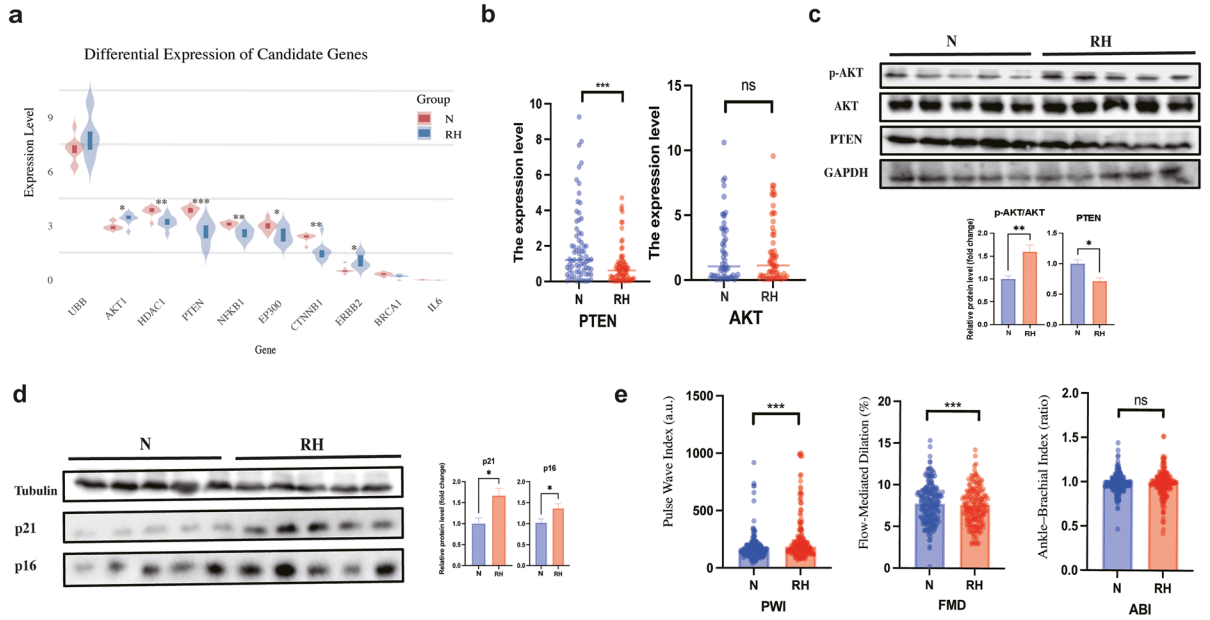


Fig. 4 Validation of PTEN–AKT-associated senescence markers and vascular function in resistant hypertension. **a** Violin plots showing differential expression of candidate hub genes in the GSE236442 dataset (Control $n=10$, RH $n=10$). **b** Quantitative RT–PCR analysis of PTEN and AKT1 expression in PBMCs from normotensive and resistant hypertension participants in the WalkByLab Brandenburg cohort (PTEN: N, $n=71$; RH, $n=74$; AKT1: N, $n=62$; RH, $n=72$). The numbers shown reflect the samples available for each target after quality control. Samples with reference gene Ct values > 25 were excluded according to predefined quality-control criteria. **c** Western blot analysis of PTEN, AKT, and p-AKT protein levels in normotensive (N) and resistant hypertension (RH) groups, confirming PTEN downregulation and AKT activation ($n=5$ per group). **d** Western blot analysis of the senescence markers p21 and p16, demonstrating increased expression in the RH group (n = 5 per group). **e** Vascular function parameters including pulse wave index (PWI), flow-mediated dilation (FMD), and ankle–brachial index (ABI) were analyzed in participants with available measurements (PWI: N, $n=213$; RH, $n=163$; FMD: N, $n=213$; RH, $n=162$; ABI: N, $n=213$; RH, $n=163$). Statistical comparisons between two groups were performed using a two-tailed Student's t-test or Mann–Whitney U test as appropriate. Vascular function parameters were analyzed using linear regression models adjusted for age, and the reported P values correspond to the age-adjusted results. $^{*}P<0.05$; $^{**}P<0.01$; $^{***}P<0.001$; ns, non-significant

selected variables were subsequently incorporated into a multivariable logistic regression model and visualized as a nomogram to facilitate individualized RH risk prediction (Fig. 6c). Calibration analysis demonstrated good agreement between the nomogram-predicted and observed probabilities (Fig. 6d), indicating satisfactory model calibration. Receiver operating characteristic (ROC) analysis further supported the model's predictive ability. The integrated model incorporating PTEN and AKT1 achieved an AUC of 0.875, compared with the baseline clinical model alone (AUC = 0.810) (Fig. 6e). Together, these findings suggest that PTEN and AKT1 may add clinically relevant information to conventional risk factors and may support future clinical–molecular risk stratification in RH, although the model should be considered preliminary until externally validated.

Discussion

In our WalkByLab cohort study (Brandenburg, Germany), patients with RH exhibited significantly higher age and BMI compared with those with essential hypertension or normotension. The nonlinear positive associations between these factors and hypertension risk indicate that older age provides a clinical context consistent with vascular aging, whereas higher BMI may reflect a clinically relevant accelerator of this process in RH. These findings are consistent with previous retrospective studies, which

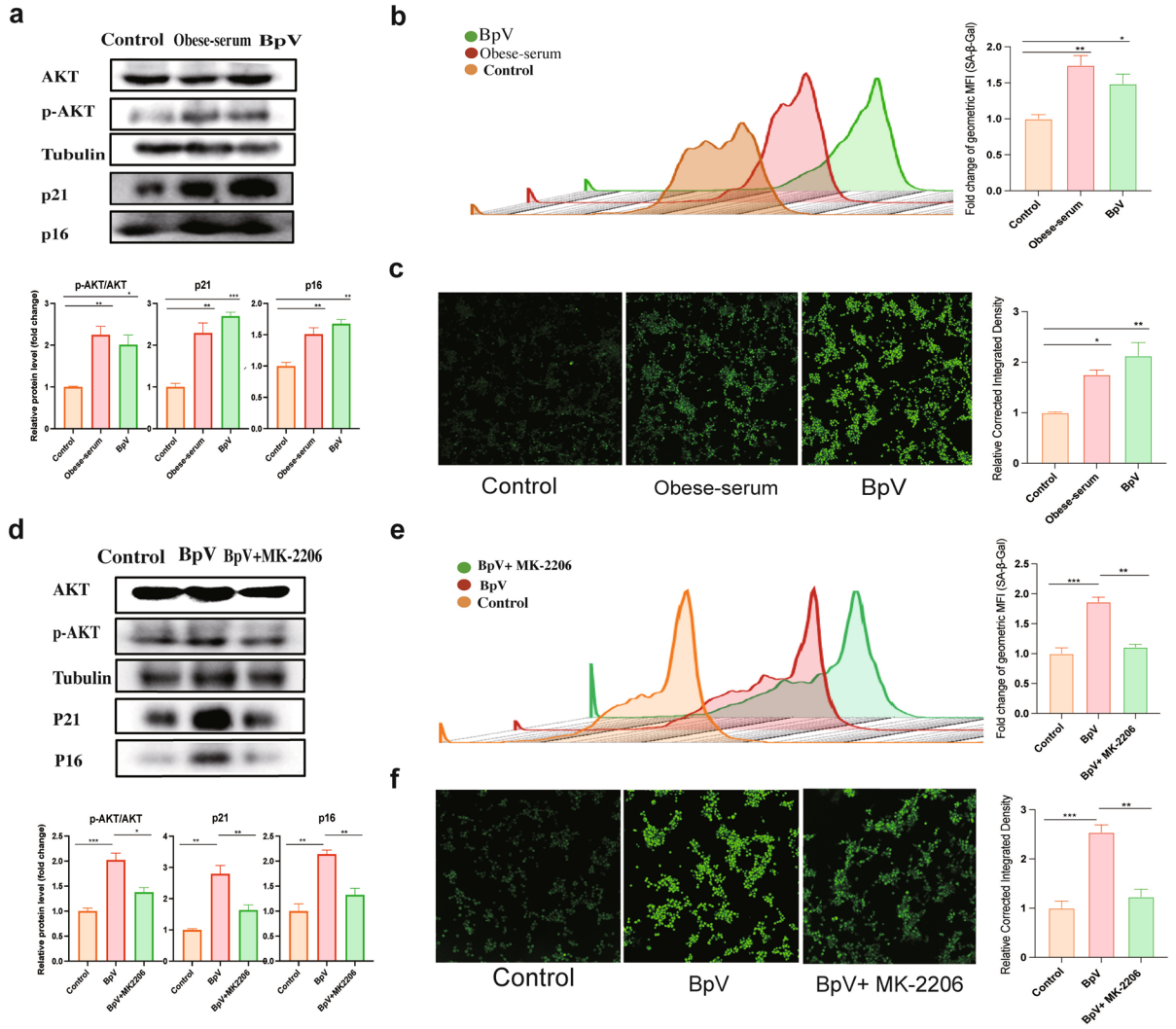


Fig. 5 Experimental assessment of PTEN–AKT signaling in endothelial senescence. **a** Western blot analysis of AKT, p-AKT, p21, and p16 expression in HUVECs cultured under standard FBS conditions, obese-serum-supplemented medium, or the PTEN inhibitor BpV. Tubulin served as the loading control. **b** Flow cytometric analysis of senescence-associated β-galactosidase (SA-β-gal) activity in the three groups, with quantitative comparison of mean fluorescence intensity (MFI). **c** Fluorescence microscopy images showing SA-β-gal staining of senescent cells under the same conditions, accompanied by quantitative analysis of fluorescence intensity. **d** Western blot analysis of AKT, p-AKT, p21, and p16 expression in HUVECs treated with BpV, with or without the AKT inhibitor MK-2206. **e** Flow cytometric analysis of SA-β-gal activity and corresponding MFI quantification for control, BpV, and BpV + MK-2206 groups. **f** Fluorescence microscopy images acquired using a 10 × objective and quantification of SA-β-gal staining intensity under the same treatment conditions. All experiments were performed with at least three independent biological replicates ($n = 3$) unless otherwise indicated. Differences among multiple groups were analyzed using one-way ANOVA followed by Tukey's post hoc test. Data are presented as mean ± SD. $^{*}P < 0.05$; $^{**}P < 0.01$; $^{***}P < 0.001$; ns, non-significant

have established that the pathogenesis of RH is multifactorial, involving obesity, arterial stiffness, chronic kidney disease, aldosterone excess, and sympathetic overactivity [1, 18]. Importantly, our vascular function data showed impaired endothelial function and increased arterial stiffness in RH. Lower FMD and higher PWI remained evident after adjustment for age, suggesting that these vascular abnormalities cannot be explained by chronological age alone. Biological vascular aging may progress differently from

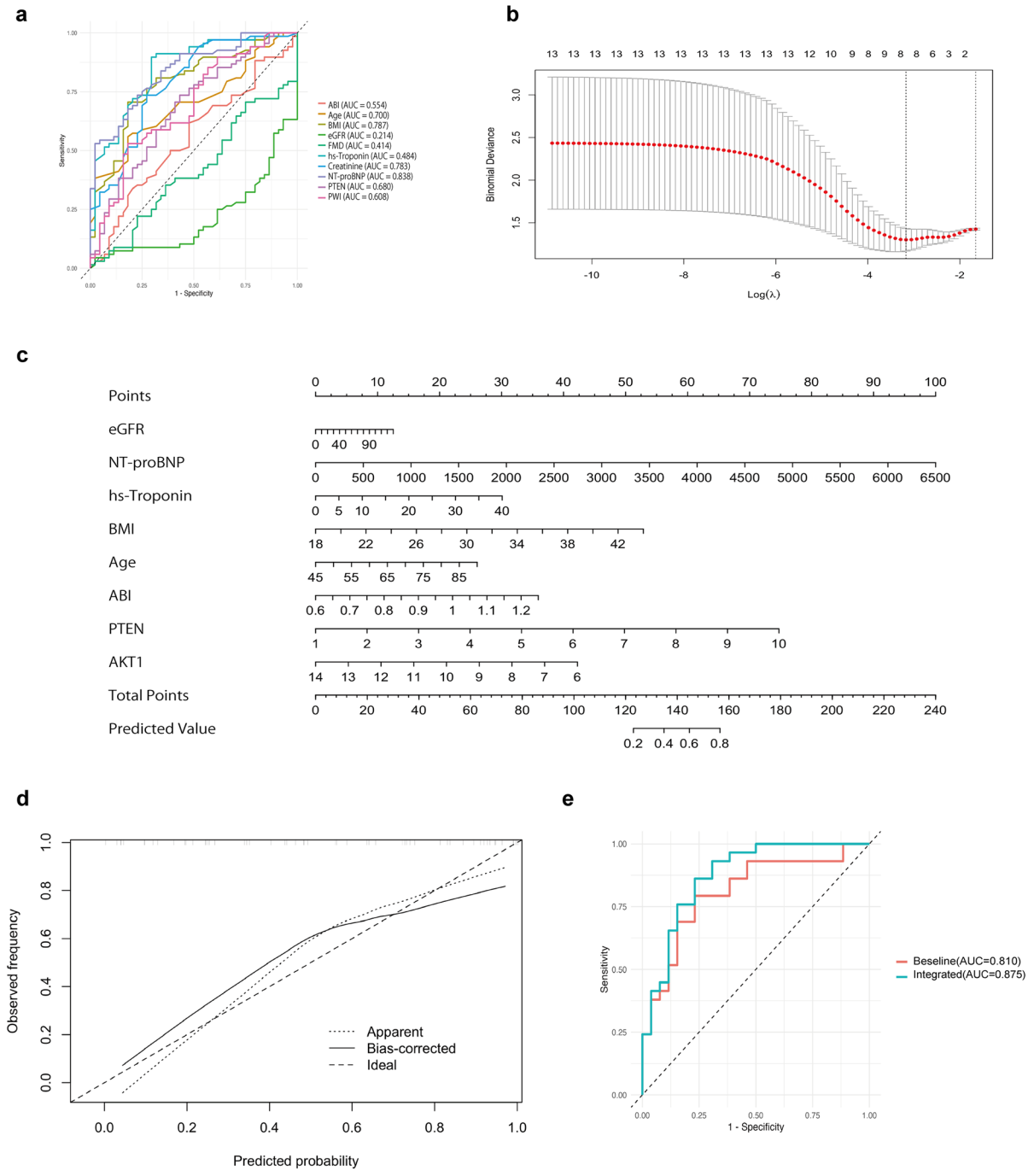


Fig. 6 Construction and evaluation of the nomogram model for resistant hypertension. **a** Receiver operating characteristic (ROC) curves of candidate clinical and molecular predictors for RH. **b** LASSO regression showing variable selection and optimal tuning parameter (λ) determined by 10-fold cross-validation. **c** Nomogram integrating clinical variables and molecular markers (PTEN and AKT1) for individualized prediction of RH risk. **d** Calibration curve assessing the agreement between predicted and observed probabilities of RH. **e** Comparison of the baseline clinical model and the integrated model including molecular markers using ROC analysis

chronological aging, with substantial differences in vascular function among individuals of similar age [19]. Together, these findings support a vascular aging–related profile in RH and raise the question of whether reduced vascular resilience may contribute to treatment resistance. With vascular aging, the ability of the endothelium to maintain homeostasis and adapt to repeated stress declines, while chronic inflammation and oxidative stress may further impair endothelial resilience [12, 20, 21]. Consistent with this concept, previous studies in RH have reported greater arterial stiffness, endothelial dysfunction, and inflammatory activation than in controlled hypertension [22]. In some patients with RH, reduced vascular resilience to sustained hemodynamic and metabolic stress may therefore accompany the established renal and neurohumoral mechanisms underlying treatment resistance [18]. Cellular senescence may contribute to this loss of vascular resilience by impairing endothelial homeostasis, reducing vascular compliance, and sustaining a pro-inflammatory vascular environment through senescence-associated signaling [23]. From a broader geroscience perspective, chronic low-grade inflammation and age-related immune dysregulation may interact with cellular senescence and endothelial dysfunction, thereby contributing to reduced vascular resilience. A clinical study in hypertension has linked senescence-associated immune changes with systemic inflammation and impaired endothelial function, suggesting that immune aging may accompany vascular dysfunction [24]. These immune-related changes may further contribute to an inflammatory and senescence-associated environment that compromises vascular homeostasis in RH. Within this framework, obesity was considered a clinically relevant context rather than the primary disease focus, as obesity-associated metabolic inflammation, oxidative stress, endothelial activation, and adipokine imbalance may accelerate vascular aging [4, 25].

To explore the molecular mechanisms underlying these clinical associations, we performed integrated transcriptomic and network analyses using three publicly available human obesity-related gene expression datasets (GSE53232, GSE87493, and GSE181339) in combination with a curated senescence-associated gene set from the Human Ageing Genomic Resources. This strategy was designed to identify obesity-associated metabolic-aging signals that converge with cellular senescence pathways implicated in vascular aging and hypertension. This approach identified a set of hub genes that link obesity-associated transcriptional alterations to aging-related signaling pathways, potentially relevant to vascular aging in RH. To determine whether these genes are also present in resistant hypertension, we first examined their expression in an independent public RH RNA-seq dataset (GSE236442). Several hub genes closely associated with obesity and cellular senescence were identified as significantly dysregulated in patients with RH, particularly PTEN, HDAC1, AKT1, NFKB1, and CTNNB1. Notably, KEGG pathway enrichment analysis based on obesity-related datasets and xCell immune profiling performed on the RH RNA-seq dataset consistently highlighted pathways and transcriptional signatures related to cellular senescence, inflammation, and immune dysregulation. These mixed immune-cell enrichment patterns are consistent with inflammatory and immune dysregulation associated with vascular aging. Experimental studies have further shown that endothelial senescence, DNA damage, and vascular inflammation are closely interconnected [23]. The PI3K–AKT signaling pathway was also enriched in these analyses, together with pathways related to vascular aging, providing a rationale for examining PTEN–AKT signaling as one candidate pathway within this broader network. Together, these findings support PTEN–AKT signaling as a candidate molecular pathway linking obesity-associated senescence signals with the vascular aging–related profile observed in RH.

Because several of the transcriptomic datasets were derived from blood samples, the observed transcriptional patterns likely reflect systemic molecular signals related to obesity-associated aging. We therefore examined PBMCs from RH patients in the WalkByLab Brandenburg cohort to determine whether the transcriptomic findings were accompanied by senescence-associated molecular alterations in circulating immune cells. RT–PCR analysis confirmed marked downregulation of PTEN. Western blotting revealed reduced PTEN expression, accompanied by increased AKT phosphorylation and elevated levels of the senescence markers p21 and p16. Together, these PBMC findings are interpreted as a systemic senescence-associated molecular profile in RH. Previous reports have linked senescence-related changes in circulating immune cells to impaired FMD in hypertension [24] and to arterial stiffness

assessed by pulse wave velocity [26], while peripheral-blood p16INK4a has been proposed as a marker of molecular aging [27]. Consistent with these observations, these molecular alterations in our cohort occurred alongside reduced FMD and increased PWI, whereas ABI remained unchanged, linking the systemic senescence-associated profile with functional vascular abnormalities consistent with vascular aging. Although these vascular assessments do not by themselves prove vascular aging, the combination of impaired endothelial vasodilatory capacity, arterial stiffening, and absence of clear evidence for advanced peripheral arterial obstruction supports the interpretation that RH is associated predominantly with functional vascular impairment rather than established occlusive vascular disease. Although AKT1 transcript levels were not significantly altered, the phosphorylated form of AKT was clearly increased. This finding suggests that persistent AKT activation, rather than increased AKT1 transcription, may contribute to the senescence response associated with PTEN reduction.

Having identified a vascular aging–related profile in RH, we next asked which molecular pathway might connect obesity-associated metabolic stress with senescence-related vascular dysfunction. We next reviewed published evidence linking PTEN dysregulation to obesity and metabolic stress. PTEN has been widely implicated in metabolic regulation related to obesity. In a cohort of 1,014 individuals with severe obesity, approximately 3% were diagnosed with monogenic obesity due to pathogenic variants in several obesity-associated genes, including PTEN [28]. Carriers of PTEN mutations typically exhibit an obese phenotype characterized by enhanced insulin sensitivity and increased adipose AKT phosphorylation, indicating that PTEN suppression drives persistent PI3K/AKT activation [29]. Another clinical study showed that PTEN expression in adipose tissue was inversely correlated with insulin resistance indices, while PI3K/AKT-related genes were positively correlated, supporting a role for PTEN in regulating lipid metabolism via PI3K/AKT inhibition [30]. Given the established link between obesity and systemic cellular senescence [31], inhibition or loss of PTEN may facilitate senescence through sustained AKT activation [32, 33]. Notably, PTEN is also involved in metabolic regulation and insulin signaling, and its expression or activity may vary depending on tissue context and disease conditions [34]. Therefore, obesity is not uniformly associated with PTEN downregulation across all biological settings.

Beyond metabolic regulation, PTEN has also been implicated in vascular aging and structural remodeling. In vascular smooth muscle cells (VSMCs), PTEN downregulation accelerates senescence by activating the PKCδ–NOX1 signaling pathway and increasing reactive oxygen species production [35]. Similarly, in primary rat VSMCs, PTEN acts as a downstream mechanotransducer of the Piezo1–miR-582-5p axis, and its inhibition activates PI3K/AKT signaling, thereby promoting senescence phenotypic alterations [36, 37]. In vivo, PTEN inhibition leads to persistent AKT activation, accompanied by vascular wall thickening, collagen deposition, and reduced compliance, features consistent with vascular remodeling and vascular aging [37]. Moreover, in smooth muscle cell–specific PTEN knockout mice, PTEN loss under high-fat diet conditions results in earlier and more pronounced collagen accumulation and structural remodeling. In human coronary artery tissues, PTEN protein expression is markedly reduced in both non-atherosclerotic and atherosclerotic lesions, with the degree of reduction closely correlated with vascular fibrosis, collagen deposition, and VSMC dedifferentiation, further linking reduced PTEN expression with human vascular remodeling [38]. Conversely, interventions that enhance PTEN expression or activity have been shown to alleviate vascular aging and prevent hypertensive vascular remodeling by maintaining the balance of the PI3K/AKT axis [39, 40]. These observations support the hypothesis that reduced PTEN expression combined with excessive AKT activity under obese conditions can drive p21/p16-mediated cellular senescence and dysfunction, thereby potentially contributing to impaired vasodilation and arterial stiffening.

Human studies further suggest that vascular dysfunction in RH develops within a broader pathophysiological context. Aldosterone excess has been associated with impaired vasodilatory function in RH [41], while mechanistic studies also support important contributions from salt and volume retention [42]. Sympathetic overactivity is also an established contributor to hypertension and has been linked to both aging and obesity-related cardiovascular dysfunction [43]. These findings indicate that endothelial dysfunction is unlikely to occur in isolation, but rather alongside other mechanisms involved in RH. Against

this background, we used HUVECs to examine the endothelial contribution of PTEN–AKT-associated senescence within this broader setting. The use of pooled obese human serum further provided a composite obesity-associated circulating stimulus, allowing the endothelial response to be examined in the presence of multiple circulating factors rather than a single defined stimulus, consistent with previous serum-based endothelial cell studies in RH and obesity [44, 45]. Exposure of HUVECs to obese human serum or pharmacological PTEN inhibition with BpV enhanced AKT phosphorylation. Our pharmacological experiments using the PTEN inhibitor BpV and the AKT inhibitor MK-2206 suggest that activation of the PTEN/AKT axis represents one relevant pathway contributing to endothelial senescence under obesity-associated conditions. These changes were accompanied by increased expression of the senescence markers p21 and p16, as well as enhanced β-galactosidase activity. Treatment with the AKT inhibitor MK-2206 partially reversed these effects by lowering p-AKT levels, reducing p21/p16 expression, and decreasing the proportion of senescent cells, supporting the involvement of AKT signaling in the senescence phenotype associated with pharmacological PTEN inhibition.

Our findings are consistent with previous mechanistic studies. In pulmonary epithelial cells, PTEN downregulation is accompanied by AKT activation and p21 upregulation [46]. In endothelial cells, decreased PTEN expression activates the PI3K/AKT/mTOR pathway and elevates p21/p16 levels [47]. Loss of PTEN predisposes cells to senescence rather than apoptosis through the AKT/ROS/p53/p21 axis [48]. Furthermore, other studies have identified PTEN as an important anti-senescence node, where upregulation of PTEN mitigates vascular smooth muscle cell aging by reducing reactive oxygen species and inhibiting Ang II-induced oxidative damage [49]. Collectively, these studies support PTEN–AKT signaling as a mechanistically relevant pathway linking senescence-related changes with endothelial dysfunction. Our findings support a model in which PTEN suppression under obesity-associated stress enhances AKT signaling, promotes p21/p16-associated cell-cycle arrest and endothelial senescence, and may thereby contribute to vascular dysfunction. Rather than acting in isolation, PTEN–AKT signaling may interact with broader stress and inflammatory pathways that contribute to vascular aging. DNA-damage responses and oxidative stress can promote p53/p21-mediated cell-cycle arrest, whereas mTOR and chronic inflammatory signaling may further reinforce senescence-associated phenotypes and endothelial dysfunction [6, 50]. These interconnected pathways may converge with PTEN–AKT signaling to contribute to the senescence-associated and vascular aging–related changes observed in RH.

Based on the above findings, we developed a predictive model integrating clinical indicators and molecular markers. Using LASSO logistic regression, both traditional cardiovascular factors and two molecular markers, PTEN and AKT1, were identified as independent predictors of resistant hypertension. The integrated model incorporating PTEN and AKT1 achieved an AUC of 0.875, compared with 0.810 for the baseline clinical model. Because the model was developed within a single cohort, external validation in independent populations will be necessary to confirm the generalizability and clinical utility of this nomogram. These findings suggest that PTEN and AKT1 may provide complementary information beyond conventional clinical variables and, with further validation, contribute to future patient stratification and clinical decision-making in RH.

The contribution of the present study lies in linking age-adjusted vascular dysfunction with systemic senescence-associated molecular changes and concordant endothelial responses within the specific context of RH. Rather than identifying a new senescence pathway, our findings position PTEN–AKT-associated cellular senescence as one mechanistically relevant component of a broader vascular aging process in RH. The exploratory clinical–molecular model provides an initial link between these biological findings and future patient stratification as additional independent data become available. Viewed together, the systemic senescence-associated molecular profile, age-adjusted vascular functional abnormalities, and endothelial-cell findings support a coherent vascular aging–related pattern in RH across clinical, molecular, and experimental levels. This convergence supports the concept that a vascular aging–enriched phenotype may be identifiable within the heterogeneous RH population and provides a rationale for future phenotypic stratification. Such stratification could also facilitate the evaluation of senescence-modulating

strategies, which have improved vascular function in experimental aging models [23].

Several limitations should be acknowledged in this study. First, the sample size was relatively small, which may limit the generalizability of our findings. Second, the retrospective observational design cannot determine causal relationships between vascular aging, cellular senescence, and RH. A fully standardized protocol to exclude pseudo-resistant hypertension was not uniformly available for all participants. Therefore, some degree of misclassification cannot be completely excluded. Although endothelial dysfunction and arterial stiffness remained evident after adjustment for age, the present findings support a vascular aging–related profile rather than a formally defined accelerated vascular aging phenotype. Longitudinal studies incorporating vascular function and biological aging will be important to establish whether this profile identifies a reproducible subgroup within RH.

Because the molecular analyses were performed in bulk PBMCs, the observed PTEN–AKT and senescence-associated changes cannot be attributed to a specific immune-cell population and may partly reflect differences in PBMC composition. These findings therefore represent a systemic circulating-cell profile rather than endothelial-cell-specific signaling. Future studies of defined immune-cell subsets may help identify the main cellular sources of these changes. The pharmacological findings support the involvement of PTEN–AKT signaling but do not establish PTEN-specific causality. HUVECs are venous endothelial cells and may not fully reproduce the phenotype of adult arterial or resistance-vessel endothelium relevant to blood-pressure regulation. Moreover, the short-term serum and pharmacological exposures capture acute senescence-associated responses rather than the cumulative vascular effects of long-standing hypertension and aging, while serum pooling may attenuate inter-individual biological variability. A lean-serum comparator was not included. Therefore, obese-serum-containing conditions should be interpreted as a model of obesity-associated circulating stress rather than definitive evidence of obesity-specific causality. The specific metabolic, inflammatory, or circulating mediators linking obesity-associated stress to endothelial senescence and vascular dysfunction were not dissected and warrant further investigation.

Conclusion

This study provides a translational framework that integrates epidemiological, transcriptomic, molecular, vascular-function, and endothelial-cell evidence to characterize vascular aging–related clinical and molecular features in resistant hypertension and to identify PTEN–AKT-associated cellular senescence as a potential mechanistic link between obesity-associated stress, vascular dysfunction, and RH. Across public datasets, PBMC samples, and in vitro models, the consistent pattern of reduced PTEN expression and enhanced AKT signaling supports PTEN–AKT-associated cellular senescence as a mechanistically relevant pathway linking obesity-associated stress with vascular dysfunction in RH. Incorporating PTEN and AKT1 into a clinical–molecular nomogram further suggested that these markers may add clinically relevant information to conventional risk factors. At a broader biological level, age-adjusted vascular dysfunction, systemic senescence-associated molecular changes, and concordant endothelial-cell findings together support the concept that accelerated vascular aging may represent an important biological dimension of RH. This pattern further raises the possibility that a vascular aging–enriched subgroup may exist within the heterogeneous RH population and could form the basis for future phenotypic stratification.

Author Contribution All authors made a significant contribution to the work reported, whether in the conception, study design, execution, acquisition of data, analysis, and interpretation, or in all these areas; took part in drafting, revising, or critically reviewing the article; gave final approval of the version to be published; have agreed on the journal to which the article has been submitted; and agree to be accountable for all aspects of the work.

Funding Open Access funding enabled and organized by Projekt DEAL. This work was supported by the Center for Aging Research Brandenburg (ZAF-BB) at Brandenburg Medical School (MHB) through the project “Sustainable Prevention: VascularAge Score”, and by the State of Brandenburg via the StaF Verbund funding program of the Ministry of Science, Research and Culture (MWFK), co-funded by the European Regional Development Fund (ERDF).

Data availability Publicly available datasets analyzed in this study are available from the GEO database under accession numbers GSE53232, GSE87493, GSE181339, and GSE236442.

Declarations

Ethics approval and consent to participate The studies involving human participants were reviewed and approved by the Ethics Committee of the Cottbus Medical Association (Landesärztekammer Cottbus; approval number: AS 74(bB)/2018). All procedures were conducted in accordance with the principles of the Declaration of Helsinki. Written informed consent was obtained from all participants prior to their inclusion in the study.

Consent for publication Not applicable.

Conflict of interest The authors have declared no conflict of interest.

Open Access This article is licensed under a Creative Commons Attribution 4.0 International License, which permits use, sharing, adaptation, distribution and reproduction in any medium or format, as long as you give appropriate credit to the original author(s) and the source, provide a link to the Creative Commons licence, and indicate if changes were made. The images or other third party material in this article are included in the article's Creative Commons licence, unless indicated otherwise in a credit line to the material. If material is not included in the article's Creative Commons licence and your intended use is not permitted by statutory regulation or exceeds the permitted use, you will need to obtain permission directly from the copyright holder. To view a copy of this licence, visit http://creativecommons.org/licenses/by/4.0/.

References

1. Carey RM, Calhoun DA, Bakris GL, Brook RD, Daugherty SL, Dennison-Himmelfarb CR, et al. Resistant hypertension: detection, evaluation, and management: a scientific statement from the American Heart Association. Hypertension. 2018;72(5):e53–90. https://doi.org/10.1161/hyp.0000000000000084.
2. Schiffrin EL, Fisher NDL. Diagnosis and management of resistant hypertension. BMJ. 2024;385:e079108. https://doi.org/10.1136/bmj-2023-079108.
3. Daugherty SL, Powers JD, Magid DJ, Tavel HM, Masoudi FA, Margolis KL, et al. Incidence and prognosis of resistant hypertension in hypertensive patients. Circulation. 2012;125(13):1635–42. https://doi.org/10.1161/circulationaha.111.068064.
4. Herzog MJ, Müller P, Lechner K, Stiebler M, Arndt P, Kunz M, et al. Arterial stiffness and vascular aging: mechanisms, prevention, and therapy. Signal Transduct Target Ther. 2025;10(1):282. https://doi.org/10.1038/s41392-025-02346-0.
5. Saad Rodrigues CI, Roderjan CN, Bezerra da Silva JG, Muxfeldt ES. Arterial stiffness in resistant hypertension: from physiology to medical practice. Open Cardiovasc Med J. 2025;19:e18741924367372. https://doi.org/10.2174/0118741924367372250203034625.
6. Summer S, Borrell-Pages M, Bruno RM, Climie RE, Dipla K, Dogan A, et al. Centenarians-the way to healthy vascular ageing and longevity: a review from VascAgeNet. Geroscience. 2025;47(1):685–702. https://doi.org/10.1007/s11357-024-01467-8.
7. Chen MS, Lee RT, Garbern JC. Senescence mechanisms and targets in the heart. Cardiovasc Res. 2022;118(5):1173–87. https://doi.org/10.1093/cvr/cvab161.
8. Hwang HJ, Kim N, Herman AB, Gorospe M, Lee JS. Factors and pathways modulating endothelial cell senescence in vascular aging. Int J Mol Sci. 2022. https://doi.org/10.3390/ijms231710135.
9. Sun Y, Wang X, Liu T, Zhu X, Pan X. The multifaceted role of the SASP in atherosclerosis: from mechanisms to therapeutic opportunities. Cell Biosci. 2022;12(1):74. https://doi.org/10.1186/s13578-022-00815-5.
10. Chu Q, Li Y, Wu J, Gao Y, Guo X, Li J, et al. Oxysterol sensing through GPR183 triggers endothelial senescence in hypertension. Circ Res. 2024;135(7):708–21. https://doi.org/10.1161/circresaha.124.324722.
11. Ungvari Z, Tarantini S, Nyúl-Tóth Á, Kiss T, Yabluchanskiy A, Csipo T, et al. Nrf2 dysfunction and impaired cellular resilience to oxidative stressors in the aged vasculature: from increased cellular senescence to the pathogenesis of age-related vascular diseases. Geroscience. 2019;41(6):727–38. https://doi.org/10.1007/s11357-019-00107-w.
12. Zeng Y, Buonfiglio F, Li J, Pfeiffer N, Gericke A. Mechanisms underlying vascular inflammaging: current insights and potential treatment approaches. Aging Dis. 2024;16(4):1889–917. https://doi.org/10.14336/ad.2024.0922.
13. Fedorova O, Parfenyev S, Daks A, Shuvalov O, Barlev NA. The role of PTEN in epithelial-mesenchymal transition. Cancers (Basel). 2022. https://doi.org/10.3390/cancers14153786.
14. Worby CA, Dixon JE. PTEN. Annu Rev Biochem. 2014;83:641–69. https://doi.org/10.1146/annurev-biochem-082411-113907.
15. Oudit GY, Sun H, Kerfant BG, Crackower MA, Penninger JM, Backx PH. The role of phosphoinositide-3 kinase and PTEN in cardiovascular physiology and disease. J Mol Cell Cardiol. 2004;37(2):449–71. https://doi.org/10.1016/j.yjmcc.2004.05.015.
16. Bankoglu EE, Tschopp O, Schmitt J, Burkard P, Jahn D, Geier A, et al. Role of PTEN in oxidative stress and DNA damage in the liver of whole-body PTEN haplodeficient mice. PLoS ONE. 2016;11(11):e0166956. https://doi.org/10.1371/journal.pone.0166956.
17. Li A, Qiu M, Zhou H, Wang T, Guo W. PTEN, insulin resistance and cancer. Curr Pharm Des. 2017;23(25):3667–76. https://doi.org/10.2174/1381612823666170704124611.
18. Tabrizchi R. Management of drug-resistant hypertension as a heterogeneous disorder. Pharmacol Ther.

2025;271:108875. https://doi.org/10.1016/j.pharmthera.2025.108875.
19. Nilsson PM, Laurent S, Cunha PG, Olsen MH, Rietzschel E, Franco OH, et al. Characteristics of healthy vascular ageing in pooled population-based cohort studies: the global metabolic syndrome and artery REsearch consortium. J Hypertens. 2018;36(12):2340–9. https://doi.org/10.1097/hjh.0000000000001824.
20. Walczak I, Tarnawska M, Stawarska K, Braczko A, Paterek A, Rolski F, et al. Endothelial cell senescence and mitochondrial dysfunction in vascular ageing. Ageing Res Rev. 2026;118:103119. https://doi.org/10.1016/j.arr.2026.103119.
21. Forman DE, Kuchel GA, Newman JC, Kirkland JL, Volpi E, Taffet GE, et al. Impact of geroscience on therapeutic strategies for older adults with cardiovascular disease: JACC scientific statement. J Am Coll Cardiol. 2023;82(7):631–47. https://doi.org/10.1016/j.jacc.2023.05.038.
22. Figueiredo VN, Yugar-Toledo JC, Martins LC, Martins LB, de Faria AP, de Haro MC, et al. Vascular stiffness and endothelial dysfunction: correlations at different levels of blood pressure. Blood Press. 2012;21(1):31–8. https://doi.org/10.3109/08037051.2011.617045.
23. Clayton ZS, Rossman MJ, Mahoney SA, Venkatasubramanian R, Maurer GS, Hutton DA, et al. Cellular senescence contributes to large elastic artery stiffening and endothelial dysfunction with aging: amelioration with senolytic treatment. Hypertension. 2023;80(10):2072–87. https://doi.org/10.1161/hypertensionaha.123.21392.
24. Zhang G, Liu Y, Qiu Y, Zhang J, Sun J, Zhou Z, et al. Circulating senescent angiogenic T cells are linked with endothelial dysfunction and systemic inflammation in hypertension. J Hypertens. 2021;39(5):970–8. https://doi.org/10.1097/hjh.0000000000002715.
25. Kwaifa IK, Bahari H, Yong YK, Noor SM. Endothelial dysfunction in obesity-induced inflammation: molecular mechanisms and clinical implications. Biomolecules. 2020. https://doi.org/10.3390/biom10020291.
26. Yu HT, Youn JC, Kim JH, Seong YJ, Park SH, Kim HC, et al. Arterial stiffness is associated with cytomegalovirus-specific senescent CD8(+) T cells. J Am Heart Assoc. 2017. https://doi.org/10.1161/jaha.117.006535.
27. Liu Y, Sanoff HK, Cho H, Burd CE, Torrice C, Ibrahim JG, et al. Expression of $p16^{INK4a}$ in peripheral blood T-cells is a biomarker of human aging. Aging Cell. 2009;8(4):439–48. https://doi.org/10.1111/j.1474-9726.2009.00489.x.
28. Cooiman MI, Kleinendorst L, Aarts EO, Janssen IMC, van Amstel HKP, Blakemore AI, et al. Genetic obesity and bariatric surgery outcome in 1014 patients with morbid obesity. Obes Surg. 2020;30(2):470–7. https://doi.org/10.1007/s11695-019-04184-w.
29. Pal A, Barber TM, Van de Bunt M, Rudge SA, Zhang Q, Lachlan KL, et al. PTEN mutations as a cause of constitutive insulin sensitivity and obesity. N Engl J Med. 2012;367(11):1002–11. https://doi.org/10.1056/NEJMoa1113966.
30. Venniyoor A. PTEN: a thrifty gene that causes disease in times of plenty? Front Nutr. 2020;7:81. https://doi.org/10.3389/fnut.2020.00081.
31. Narasimhan A, Flores RR, Camell CD, Bernlohr DA, Robbins PD, Niedernhofer LJ. Cellular senescence in obesity and associated complications: a new therapeutic target. Curr Diab Rep. 2022;22(11):537–48. https://doi.org/10.1007/s11892-022-01493-w.
32. Jung SH, Hwang HJ, Kang D, Park HA, Lee HC, Jeong D, et al. mTOR kinase leads to PTEN-loss-induced cellular senescence by phosphorylating p53. Oncogene. 2019;38(10):1639–50. https://doi.org/10.1038/s41388-018-0521-8.
33. Wang CY, Kim HH, Hiroi Y, Sawada N, Salomone S, Benjamin LE, et al. Obesity increases vascular senescence and susceptibility to ischemic injury through chronic activation of Akt and mTOR. Sci Signal. 2009;2(62):ra11. https://doi.org/10.1126/scisignal.2000143.
34. Li YZ, Di Cristofano A, Woo M. Metabolic role of PTEN in insulin signaling and resistance. Cold Spring Harb Perspect Med. 2020. https://doi.org/10.1101/cshperspect.a036137.
35. Kim SG, Sung JY, Kang YJ, Choi HC. Fisetin alleviates cellular senescence through PTEN mediated inhibition of PKCδ-NOX1 pathway in vascular smooth muscle cells. Arch Gerontol Geriatr. 2023;108:104927. https://doi.org/10.1016/j.archger.2023.104927.
36. Zhang J, Wang X, Fu Z, Xing C, Wang Z, Yang H, et al. Long-term simulated microgravity fosters carotid aging-like changes via Piezo1. Cardiovasc Res. 2024;120(5):548–59. https://doi.org/10.1093/cvr/cvae024.
37. Wu Y, Chen Z, Zheng Z, Li X, Shu J, Mao R, et al. Tudor-SN exacerbates pathological vascular remodeling by promoting the polyubiquitination of PTEN via NEDD4-1. J Biomed Sci. 2024;31(1):88. https://doi.org/10.1186/s12929-024-01076-9.
38. Moulton KS, Li M, Strand K, Burgett S, McClatchey P, Tucker R, et al. PTEN deficiency promotes pathological vascular remodeling of human coronary arteries. JCI Insight. 2018. https://doi.org/10.1172/jci.insight.97228.
39. Lu S, Strand KA, Mutryn MF, Tucker RM, Jolly AJ, Furgeson SB, et al. PTEN (phosphatase and tensin homolog) protects against Ang II (Angiotensin II)-induced pathological vascular fibrosis and remodeling-brief report. Arterioscler Thromb Vasc Biol. 2020;40(2):394–403. https://doi.org/10.1161/atvbaha.119.313757.
40. Cui Z, Jiamei Y, Yushu Y, Xia F, Haiyan Y, Zhang D, et al. Effect of the traditional Chinese medicine Pinggan-Qianyang decoction on SIRT1-PTEN signaling in vascular aging in spontaneously hypertensive rats. Hypertens Res. 2021;44(9):1087–98. https://doi.org/10.1038/s41440-021-00682-6.
41. Nishizaka MK, Zaman MA, Green SA, Renfroe KY, Calhoun DA. Impaired endothelium-dependent flow-mediated vasodilation in hypertensive subjects with hyperaldosteronism. Circulation. 2004;109(23):2857–61. https://doi.org/10.1161/01.Cir.0000129307.26791.8e.
42. Williams B, MacDonald TM, Morant SV, Webb DJ, Sever P, McInnes GT, et al. Endocrine and haemodynamic changes in resistant hypertension, and blood pressure responses to spironolactone or amiloride: the PATHWAY-2 mechanisms substudies. Lancet Diabetes Endocrinol. 2018;6(6):464–75. https://doi.org/10.1016/s2213-8587(18)30071-8.

43. Balasubramanian P, Hall D, Subramanian M. Sympathetic nervous system as a target for aging and obesity-related cardiovascular diseases. Geroscience. 2019;41(1):13–24. https://doi.org/10.1007/s11357-018-0048-5.
44. Barbaro NR, de Araújo TM, Tanus-Santos JE, Anhê GF, Fontana V, Moreno H. Vascular damage in resistant hypertension: TNF-alpha inhibition effects on endothelial cells. Biomed Res Int. 2015;2015:631594. https://doi.org/10.1155/2015/631594.
45. Skilton MR, Sieveking DP, Harmer JA, Franklin J, Loughnan G, Nakhla S, et al. The effects of obesity and non-pharmacological weight loss on vascular and ventricular function and structure. Diabetes Obes Metab. 2008;10(10):874–84. https://doi.org/10.1111/j.1463-1326.2007.00817.x.
46. Qiu T, Tian Y, Gao Y, Ma M, Li H, Liu X, et al. PTEN loss regulates alveolar epithelial cell senescence in pulmonary fibrosis depending on Akt activation. Aging (Albany NY). 2019;11(18):7492–509. https://doi.org/10.18632/aging.102262.
47. He B, Shao B, Cheng C, Ye Z, Yang Y, Fan B, et al. MiR-21-mediated endothelial senescence and dysfunction are involved in cigarette smoke-induced pulmonary hypertension through activation of PI3K/AKT/mTOR signaling. Toxics. 2024. https://doi.org/10.3390/toxics12060396.
48. Lee JJ, Kim BC, Park MJ, Lee YS, Kim YN, Lee BL, et al. PTEN status switches cell fate between premature senescence and apoptosis in glioma exposed to ionizing radiation. Cell Death Differ. 2011;18(4):666–77. https://doi.org/10.1038/cdd.2010.139.
49. Kim HJ, Ham SA, Kim MY, Hwang JS, Lee H, Kang ES, et al. PPARδ coordinates angiotensin II-induced senescence in vascular smooth muscle cells through PTEN-mediated inhibition of superoxide generation. J Biol Chem. 2011;286(52):44585–93. https://doi.org/10.1074/jbc.M111.222562.
50. Han Y, Kim SY. Endothelial senescence in vascular diseases: current understanding and future opportunities in senotherapeutics. Exp Mol Med. 2023;55(1):1–12. https://doi.org/10.1038/s12276-022-00906-w.

Publisher's Note Springer Nature remains neutral with regard to jurisdictional claims in published maps and institutional affiliations.